

Tribological characteristics and micromilling performance of nanoparticle enhanced water based cutting fluids in minimum quantity lubrication

A. Sravan Kumar*, Sankha Deb, S. Paul

Machine Tool and Machining Lab, Department of Mechanical Engineering, Indian Institute of Technology Kharagpur, West Bengal, 721302, India

ARTICLE INFO

Keywords:
Nanofluids
Solid lubricant
Minimum quantity lubrication
Ball-on-disk tribometry
Friction
Micromilling

ABSTRACT

Friction and wear characteristics of water-based nanofluids were studied. Deionized water-based nanofluids were prepared with alumina (Al_2O_3), hBN, MoS_2 , and WS_2 nanoparticles. Tribological study of the prepared nanofluids was undertaken on a ball-on-disk tribometer in minimum quantity lubrication (MQL) mode on Ti-6Al-4V workpiece. The effect of flow rate on the coefficient of friction (μ) and wear of the workpiece was reported for different nanofluids. 3D profiles of the wear tracks were obtained to study the wear depth and wear profile. Alumina-based nanofluids have shown excellent performance in terms of friction and wear as compared to the other nanofluids. The coefficient of friction, wear track depth and specific wear were reduced by 53.89 %, 23.4 %, and 37.03 % respectively for alumina nanofluid in MQL mode as compared to the dry environment. A commercial cutting fluid (UNILUB 2032) was used for comparative studies. The commercial cutting fluid performed slightly better than the alumina nanofluid, both used in MQL mode. Even though hBN, MoS_2 , and WS_2 are solid lubricants, their performance as nanofluids in MQL mode was not better than alumina nanofluids. Alumina particles, being spherical shaped, were able to provide better lubrication owing to the ball-bearing effect. Scanning electron microscopy (SEM) and energy dispersive X-ray spectroscopy (EDS) of the wear tracks were conducted to understand the mechanism of friction and wear reduction. Micromilling experiments were done on Ti-6Al-4V using the prepared cutting fluids in MQL mode to evaluate their effect on machining forces and burr formation. Alumina nanofluids and the commercial lubricant have shown significant reduction in machining forces and burr formation as compared to the other nanofluids. This is in correlation to the tribological performance of these cutting fluids.

Introduction

The demand for miniature sized components has increased rapidly in the last few decades in the fields of electronics, automotive, medicine, aerospace, communications, etc. Mechanical micro machining processes like micromilling have distinct advantages over lithography and laser-based techniques like the ability to machine complex 3D features on both metallic and non-metallic materials with high precision [1], and the ability to machine high aspect ratio structures like thin walls [2]. The formation of burrs in mechanical machining processes is a well-known phenomenon and is a challenge in micromilling since the relative size of the burrs to the dimensions of the component is large

[3,4], and these burrs negatively affect the quality and functionality of the final product. This is mainly due to the dominance of ploughing, rubbing, and plastic deformation in the material removal process [5] arising as a result of size effects at the micro-scale [6].

Minimisation and control of burr formation in micromachining has gained increased importance due to the wide range of applications of these processes. Lee and Dornfeld [3] have reported that in micromilling, built-up edge tends to remain on the tool for longer and the rate of wear decreases as the cutting velocity increases, thereby decreasing the burr size. Lee and Dornfeld [7] have further studied the burr formation in micromilling of aluminium and copper and reported that most of the burrs formed are top burrs. Cheng et al. [8] have studied the

Abbreviations: v_c , cutting velocity (m/min); f_z , feed per flute (μm); a , depth of cut (μm); μ , coefficient of friction; F_x , feed force (N); F_y , transverse force (N); F_z , thrust force (N); σ , flow stress (MPa); ϵ , plastic strain; $\dot{\epsilon}$, strain rate (s^{-1}); $\dot{\epsilon}_0$, reference strain rate (s^{-1}); T, workpiece temperature; T_0 , room temperature; T_m , workpiece melting temperature; γ_0 , orthogonal rake angle; β , shear angle; Δy , adiabatic shear band thickness; MQL, minimum quantity lubrication; TEM, transmission electron microscope; SEM, scanning electron microscope; EDS, energy-dispersive X-ray spectroscopy; SDS, sodium dodecyl sulphate; PVP, polyvinylpyrrolidone; DI, deionised water

* Corresponding author.

E-mail address: sravan.ammiraju@iitkgp.ac.in (A.S. Kumar).

<https://doi.org/10.1016/j.jmapro.2020.05.032>

Received 9 September 2019; Received in revised form 19 May 2020; Accepted 21 May 2020

1526-6125/ © 2020 The Society of Manufacturing Engineers. Published by Elsevier Ltd. All rights reserved.

top burr formation in micromilling of Ti-6Al-4 V and have observed that the downmilling burrs were larger than the upmilling burrs. They have also reported that the burr size can be significantly reduced when the feed rate is sufficiently larger than the maximum uncut chip thickness.

The use of metalworking fluids has been integral to the metal cutting processes since these fluids aid in improving product quality and increased productivity. Flood cooling has several advantages like reducing tool wear, chip-tool interface temperature, work-tool interface friction, and surface damage on the workpiece. However, these fluids also pose problems related to the environment, human health, higher cost of handling and disposal of cutting fluids, and a need for sustainable manufacturing [9,10]. Hence, researchers have turned to sustainable alternatives like minimum quantity lubrication (MQL). In MQL, a small amount of cutting fluid is atomized, mixed with compressed air, and directly applied to the machining zone effectively [11]. Sun et al. [12] have compared MQL and flood cooling using soluble oil while end milling Ti-6Al-4 V. They have reported that MQL achieves the best lubricating effect, thereby resulting in a reduction of machining forces and tool wear.

Titanium alloys have certain unique properties like high strength to weight ratio, high-temperature strength, fracture toughness, and good corrosion resistance which has resulted in the being widely used in the fields of aerospace, bio-medical, defence, etc [13]. But these alloys are considered difficult-to-machine due to high chemical reactivity with the tool materials [14]. This has led to increased research to improve the machinability of titanium and its alloys. Vazquez et al. [15] have studied the effect of different cooling and lubrication conditions during the micromilling of Ti-6Al-4 V. They have reported that MQL has offered the best dimensional accuracy of the micro-channels whereas flood cooling produced a dimensional error of 20 %. They have also observed that MQL has resulted in better surface finish as compared to flood cooling. Ziberov et al. [16] have studied the effect of the application of cutting fluid on the tool wear, burr formation, and machined surface during micromilling of Ti-6Al-4 V. They have reported that MQL has led to an absence of built-up edge which resulted in a reduction in burr formation and surface roughness while increasing the tool wear.

The addition of nanometer-sized particles to the traditional metalworking fluids has several advantages. These “nanofluids” are known to be better than the pure fluids in terms of heat transfer coefficient [17,18], coefficient of friction [19–22], viscosity, density [23], and load-bearing capacity [20,22,24]. A lot of research is being carried out to assess the role of nanofluids in lubrication. Nanofluids have shown superior anti-friction and anti-wear properties as compared to conventional lubricants. Spherical nanoparticles like alumina (Al_2O_3), CuO, and diamond act as nano ball-bearings, thereby reducing the friction between sliding components [19,21,22]. These nanoparticles also get entrapped in the surface asperities of the workpiece, thereby strengthening the lubrication film created by the base fluid [20,20,21,22]. Solid lubricant based nanoparticles like hBN, MoS_2 , and WS_2 impart lubricating properties to the base fluids as these particles have a graphite-like lamellar structure with layers able to slide over one another, thereby reducing friction [25,26]. These nanofluids, when used as cutting fluids in MQL mode, have shown superior performance as compared to conventional cutting fluids in terms of machining forces, temperature, surface finish, and tool wear. Liao et al. [27] have studied the effect of nanofluid MQL and flood cooling in the grinding of Ti-6Al-4 V. They have reported that the grinding forces, coefficient of friction, and wheel loading have reduced in the case of nanofluid MQL. Setti et al. [28] have studied the performance of MQL using water-based Al_2O_3 and CuO nanofluids during the grinding of Ti-6Al-4 V. They have reported that the addition of nanoparticles has improved the lubricity of the cutting fluids, reduced the grinding temperature, and improved the grindability of the work material. Kim et al. [29] have studied the performance of nanodiamond MQL during micro end milling of Ti-6Al-4 V. They have reported that the addition of nanodiamond particles has enhanced the lubricating effect of the cutting fluid which resulted in

significant reduction in burr formation and surface roughness.

Past literature has discussed the mechanism of lubrication using different lubricants like synthetic oils, nanofluids with spherical nanoparticles, and solid lubricant based nanoparticles in conventional flood cooling mode. But the lubricating mechanism of these fluids in MQL mode has not been studied much. Further, limited literature is available on the correlation between the anti-friction and anti-wear properties of these fluids and the mechanism of burr formation in micromilling. Very few studies have been reported on the application of solid lubricant based nanofluids in MQL mode in micromilling. The present study is aimed at evaluating the anti-friction and anti-wear properties of water-based alumina, hBN, MoS_2 , and WS_2 nanofluids in MQL mode using ball-on-disk tribometer. None of the four nanopowders (Al_2O_3 , hBN, MoS_2 , WS_2) used in the present study are known to cause any negative ecological impact and are completely stable. Further, they are not known to have any toxic effects on long term exposure [30–33]. A commercial lubricant (UNILUB 2032) has been tested for comparison purposes. Further, the effectiveness of these nanofluids in reducing the machining forces and burr formation in micromilling of Ti-6Al-4 V alloy has been studied.

Materials and methods

Preparation of nanofluids

Alumina (Al_2O_3), hBN, MoS_2 , and WS_2 nanoparticles (Nanoshel, India) of average particle size less than 100 nm were dispersed in deionized water using an ultrasonic probe sonicator (PCI Analytics, India). Transmission electron microscope (TEM) images of the nanoparticles are shown in Fig. 1. Alumina particles are spherical in shape and hBN, MoS_2 , and WS_2 have a layered structure. The properties of the nanoparticles are shown in Table 1. Dispersion was carried out for one hour at a sonication frequency of 20 kHz and a power of 300 W at a constant temperature of 25 °C. Several surfactants were tested to stabilise the dispersions like sodium dodecyl sulphate (SDS), polyvinylpyrrolidone (PVP), cetrimonium bromide (CTAB), and sodium dodecylbenzene sulfonate (SDBS). Out of the tested surfactants, SDS was found to be the best for alumina, MoS_2 , and WS_2 nanofluids, and PVP was found to be the most suitable for hBN nanofluids. Stability of the dispersions was assessed visually by observing the nanofluids 24 h

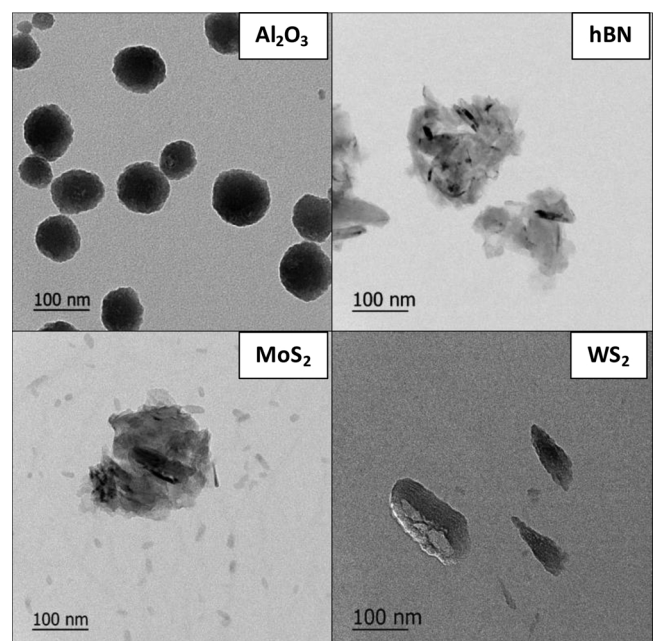


Fig. 1. TEM images of the as-received nanoparticles.

Table 1
Properties of the nanoparticles as provided by the manufacturer.

Property	Al ₂ O ₃	hBN	MoS ₂	WS ₂
Purity	99 %	> 99 %	99.9 %	> 99 %
Average particle size (nm)	< 100	70–80	80–100	80–100
Specific surface area (m ² /g)	15–20	NA	NA	80
Crystal structure	cubic	hexagonal	hexagonal	hexagonal
True Density (g/cm ³)	3.65	2.29	4.8	7.5
Thermal conductivity (W/m K)	30	20	35	32

after preparation as shown in Fig. 2. A synthetic ester-based commercial lubricant (UNILUB 2032) has also been used for studying its suitability as a cutting fluid in comparison to the prepared nanofluids. UNILUB 2032 is a non-water soluble lubricant consisting of a mixture of esters, manufactured from natural fatty acids (> C16) and sterically hindered alcohol. Composition of the prepared nanofluids is shown in Table 2.

Table 2
Composition of the prepared nanofluids.

Nanofluid	Composition
MQL Al ₂ O ₃	1% Al ₂ O ₃ + 1% SDS in DI water
MQL hBN	1% hBN + 0.1 % PVP in DI water
MQL MoS ₂	1% MoS ₂ + 1% SDS in DI water
MQL WS ₂	1% WS ₂ + 1% SDS in DI water
MQL UNILUB	UNILUB 2032 (pure MQL)

Minimum quantity lubrication (MQL) setup

Tribology experiments and subsequent micromilling experiments were conducted in dry and MQL environments. An MQL setup developed in-house has been used for this purpose. Schematic of the MQL setup is shown in Fig. 3. The system comprises an air compressor, a pressure regulator, a medical-grade syringe infusion pump (Life Plus

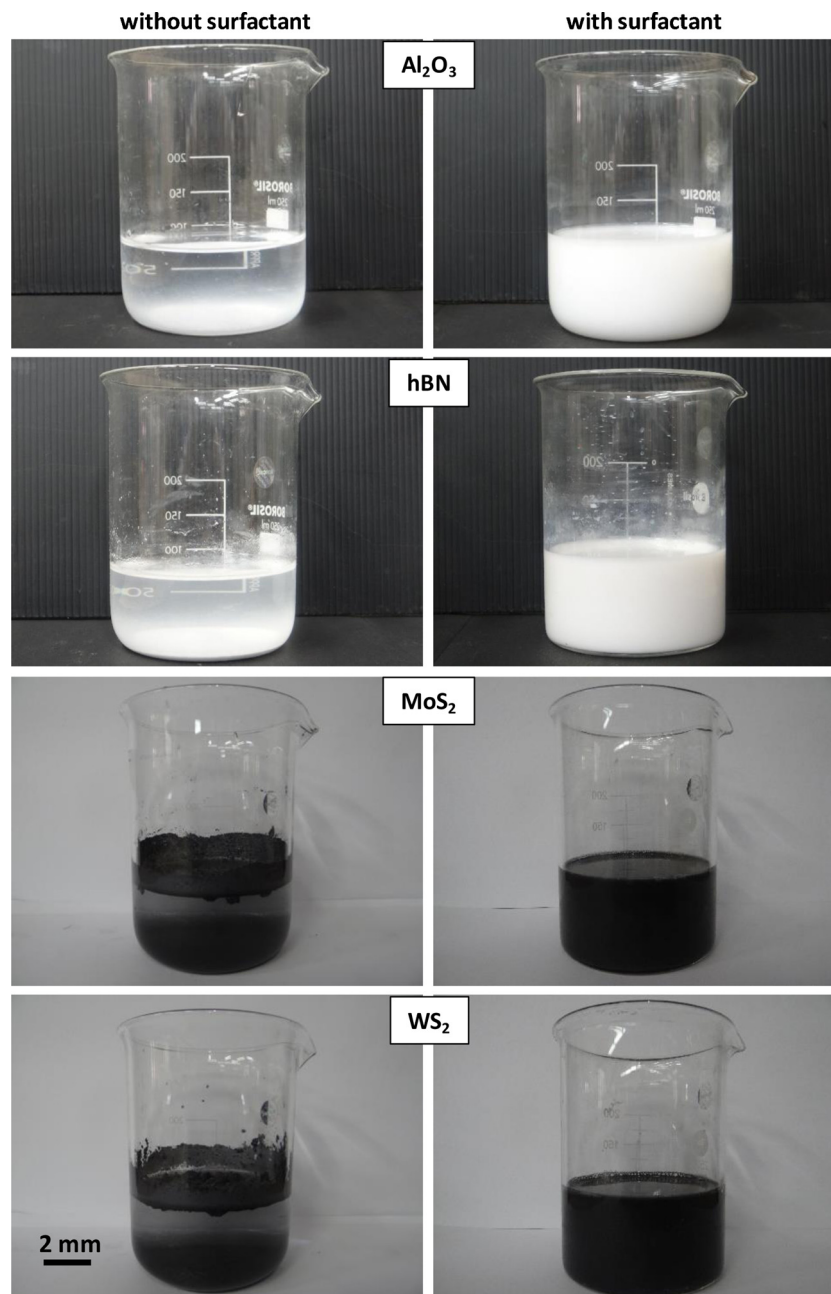


Fig. 2. Photographs of the prepared nanofluids after 24 h showing the stability of the dispersions without and with surfactant.

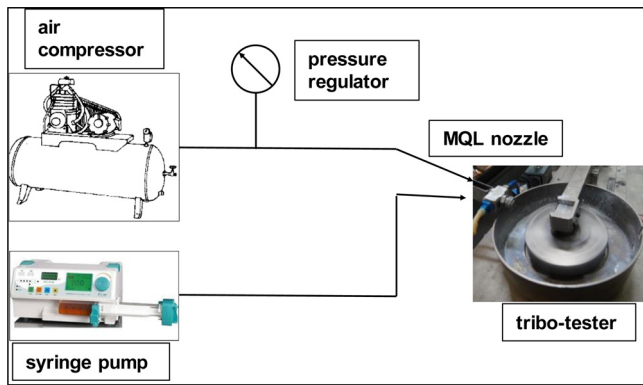


Fig. 3. Schematic of the in-house built MQL setup.

50DN, India), and an external mix nozzle (Spraying Systems Co, U.S.A, angle of divergence – 18°). Syringe infusion pump (Life Plus 50DN) has been used to supply the cutting fluid at the desired flow rate. Flow rate of the pump is user-programmable and has a range of 1 ml/hr to 1000 ml/hr with a high precision of 1 ml/hr. Cutting fluid and pressurised air were mixed in the external mix nozzle (Spraying Systems Co, fluid orifice dia. – 0.51 mm, air orifice dia. – 1.62 mm) and the atomised fluid-air mixture was supplied to the application zone. The nozzle can deliver up to 164 l/min of air at a pressure of 6.7 bar, and a liquid pressure of 3 bar. The nozzle is capable of delivering the fluid-air mixture to a distance of 250 mm without inducing turbulence in the flow.

Tribology experiments

Tribology experiments were conducted to evaluate the friction and wear properties of the prepared nanofluids using a ball-on-disk tribometer (TR 20 – M24, DUCOM, India). The experimental setup is shown in Fig. 4. Atomising air pressure was 4.5 bar and three flow rates of fluids 6 ml/hr, 50 ml/hr, and 100 ml/hr were used. Sintered and polished tungsten carbide cobalt ball of 6 mm diameter (average surface roughness – 37 nm) was used as the counter-body. Rolled Ti-6Al-4 V plates of dimensions 20 mm × 20 mm × 10 mm were used as disks. The plates were face milled on both the 20 mm × 20 mm sides and polished to achieve an average surface roughness of 44 nm. Mechanical properties of the ball and disk are given in Table 3. The counter-body was slid against the disk under a constant normal load of 10 N (nominal contact pressure of 1.37 GPa between the sliding surfaces as calculated

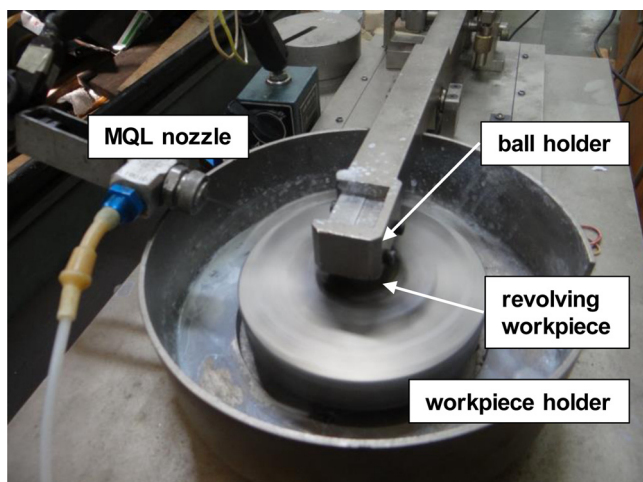


Fig. 4. Tribology experimental setup showing the tungsten carbide ball holder, revolving workpiece, and the MQL nozzle.

Table 3

Mechanical properties of ball and disk materials.

Property	Ball (WC-Co)	Disk (Ti-6Al-4 V)
Density (g/cm ³)	15.7	4.43
Young's Modulus (GPa)	696	113.8
Poisson's ratio	0.22	0.342
Hardness, Vicker's (HV100)	1730	349

using Hertzian contact theory [34]) while the disk was rotating at a constant speed of 320 rpm. Diameter of the wear track was 10 mm. MQL nozzle was positioned against the direction of motion of the ball relative to the disk. Distance between the nozzle and the sliding zone was 20 mm and the angle between the nozzle and the workpiece was 15°. Experiments were conducted for a sliding time of 20 min at ambient temperature. Two repetitions were conducted for each experimental condition. Friction force was continuously measured throughout the tribo test with the help of an inbuilt load cell. The coefficient of friction, which is a ratio of the friction force to the normal force, was determined using the measured friction force values.

After the tribology experiments, the worn workpieces were cleaned in an ultrasonic bath with acetone for one hour and dried. Volumetric wear was measured using 3D contact-type surface profilometer (Taylor Hobson Form TalySurf 50). An area of 2 mm × 4 mm was scanned to obtain the 3D profile of the wear tracks as shown in Fig. 5a. Orthogonal profiles of the wear tracks were obtained by extracting profiles of the wear track in the radial direction. Area of cross-section and the maximum depth of the wear track was measured by analysing the extracted profiles using a surface profilometry software (TalyMap Gold). Fig. 5b shows the typical cross-section of a wear track depicting the measurement of wear depth and cross-sectional area of the track. Cross-sectional profiles were analysed at different locations on the wear track and the measurements were averaged. The surfaces of the wear tracks were studied under a scanning electron microscope (SEM) (Zeiss EVO 18) to evaluate surface morphology and surface damage under different environments. Energy dispersive X-ray spectroscopy (EDS) of the wear tracks was conducted to assess any residue of the lubricants.

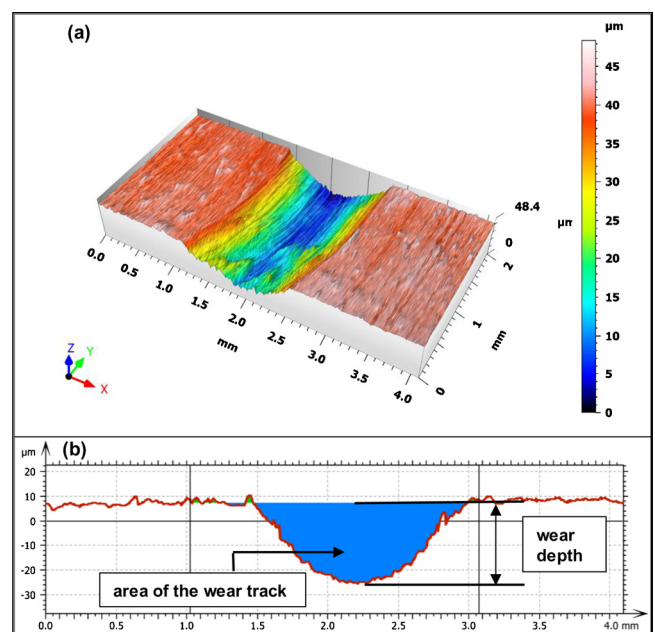


Fig. 5. Typical profilometry of the wear tracks showing (a) 3d profile; (b) cross-section of the wear track showing wear depth and area of the wear track.

Table 4
Specifications of the micro end milling cutters.

Specification	Value
Diameter	500 μm
Grain size	< 1 μm
Flute length	1 mm
Helix angle	30°
Rake angle	13° \pm 0.9°
Edge radius	2 – 3 μm
Tool coating	TiAlN

Micromilling experiments

Micromilling experiments were conducted to evaluate the machining performance of the prepared nanofluids in minimum quantity lubrication (MQL) mode. Ti-6Al-4 V plates of dimensions 20 mm \times 20 mm \times 10 mm were used as disks. The plates were face milled on both the 20 mm \times 20 mm sides and polished to achieve a parallelism of 0.075 $\mu\text{m}/\text{mm}$ and an average surface roughness of 44 nm. Two-flute tungsten carbide flat end milling cutters (E9661, AXIS Microtools, India) of 500 μm diameter were used for milling. Specifications of the tools are given in Table 4. Micro-channels of width 500 μm were milled on the prepared samples with a high precision CNC micromachining centre (Kern Evo). The prepared nanofluids were supplied to the machining zone using the in-house made MQL setup described earlier. Machining setup is shown in Fig. 6. MQL nozzle was positioned against the direction of the workpiece feed as shown in Fig. 6. Distance between the nozzle and the sliding zone was 20 mm and the angle between the nozzle and the workpiece was 15°. Two sets of parameter combinations were used for machining consisting of two levels of cutting velocities (10 m/min and 60 m/min). The feed used was 6 $\mu\text{m}/\text{flute}$, the depth of cut was 25 μm and the channel length was 5 mm. Two such channels were machined for each parametric combination to ensure test repetition.

Machining forces in three directions were measured using a three-component piezoelectric dynamometer (KISTLER 9119AA2). The dynamometer was connected to three charge amplifiers (KISTLER 5015), which were in turn connected to a digital storage oscilloscope (Agilent InfiniVision DSO-X 2014A) to store and analyse the cutting force measurements. The measured forces are analysed in MATLAB (version R2014a). Samples were cleaned in acetone in an ultrasonic bath. SEM micrographs of the machined channels were taken and analysed to measure the top burr width on both downmilling and upmilling sides of the channels. Measurements were taken at several points along the

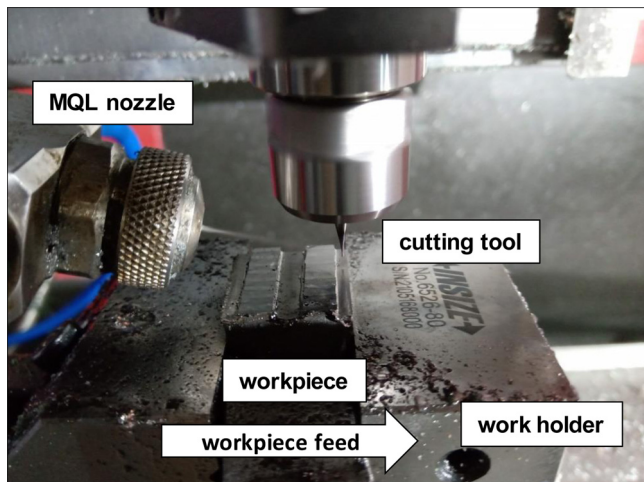


Fig. 6. Micromilling setup showing the cutting tool, workpiece, and the MQL nozzle.

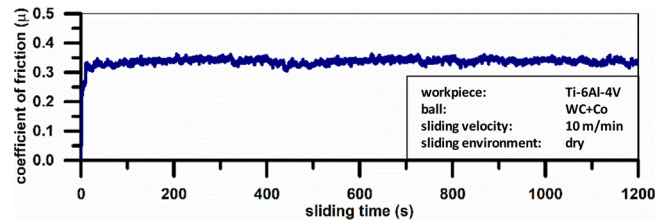


Fig. 7. Typical curve showing the variation in coefficient of friction with sliding time for dry sliding.

length of the channels and averaged to obtain accurate readings. EDS of the channels was conducted to identify the presence of lubricant residue.

Results and discussions

Tribology experiments

Fig. 7 shows a typical variation in the coefficient of friction with the sliding time. The average coefficient of friction under different lubricating conditions is shown in Fig. 8. Error bars in Fig. 8 represent the range of the values. It is observed that the coefficient of friction is maximum when no lubricant is used. The coefficient of friction decreases with the application of lubricant. The commercial lubricant has resulted in the least coefficient of friction at all flow rates. This can be attributed to the lower friction and lower wear of the ester tribofilm formed by the commercial lubricant as compared to the water-based fluids [35–37]. Alumina nanofluids have performed better than the other nanofluids and their effect on reducing the coefficient was very close to that of the commercial lubricant (10.2 % at 6 ml/hr, 5.49 % at 50 ml/hr, and 11.48 % at 100 ml/hr higher than the commercial lubricant). An increase in the flow rate leads to a reduction in the coefficient of friction for all the fluids tested. This can be attributed to the increased tribofilm stability at higher flow rates and also the availability of more nanoparticles at higher flow rates, both of which tend to reduce the sliding friction [19,20,22]. At 100 ml/hr, reduction in the coefficient of friction for alumina nanofluid and the commercial lubricant are 53.89 % and 59.19 % respectively as compared to dry friction. Alumina nanoparticles, due to their spherical shape, cause a nano ball-bearing effect between the sliding surfaces, thereby converting the friction mechanism from sliding friction to rolling friction and reducing friction [19,22]. Further, alumina nanoparticles get trapped in the asperities of the workpiece surface, thereby

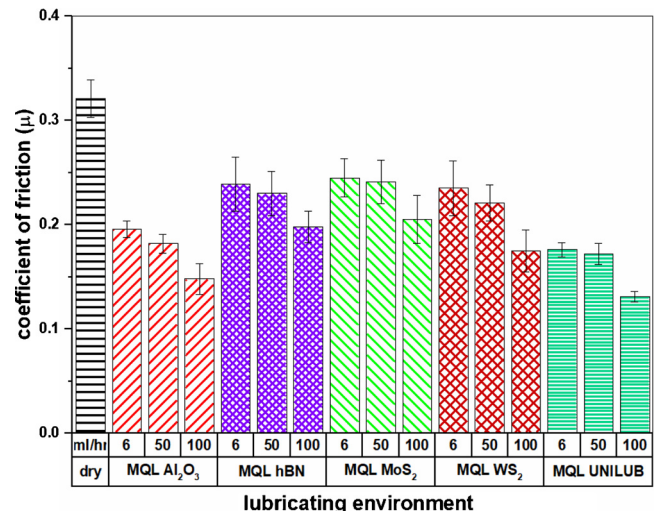


Fig. 8. Variation in the coefficient of friction at different lubricating conditions.

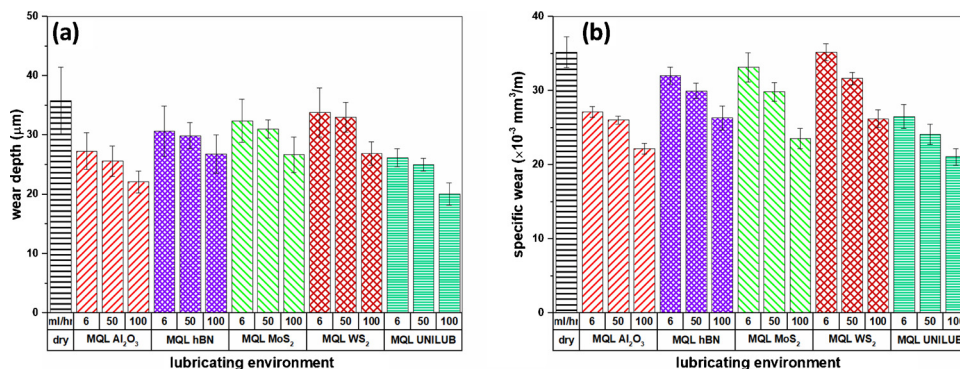


Fig. 9. Variations in (a) depth of wear track and (b) specific wear at different lubricating conditions.

strengthening the lubrication film and lowering the coefficient of friction [20–22]. This can be confirmed from the elemental composition of the wear surfaces by EDS as shown in Fig. 10. Another aspect of the nanoparticles is that they act as a third-body [20,22,24], meaning that the nanoparticles act as load-bearing bodies, thereby reducing direct contact between the sliding surfaces and reducing friction. Solid lubricant based nanofluids (hBN, MoS₂, WS₂) performed worse than alumina nanofluids at all flow rates. Mao et al. have also reported that alumina nanofluids displayed better anti-friction and anti-wear

properties than MoS₂ nanofluids [13].

Fig. 9a shows the depth of the wear track and Fig. 9b shows the specific wear under different lubricating conditions. Measurements have been recorded at six different locations on each wear track and the averages for the wear track depth and the specific wear are plotted. Error bars represent the standard deviation. It is evident from the plots that maximum wear was achieved under the dry environment. The variations in wear track depth and specific wear under different lubricating conditions follow a trend that can be correlated to the

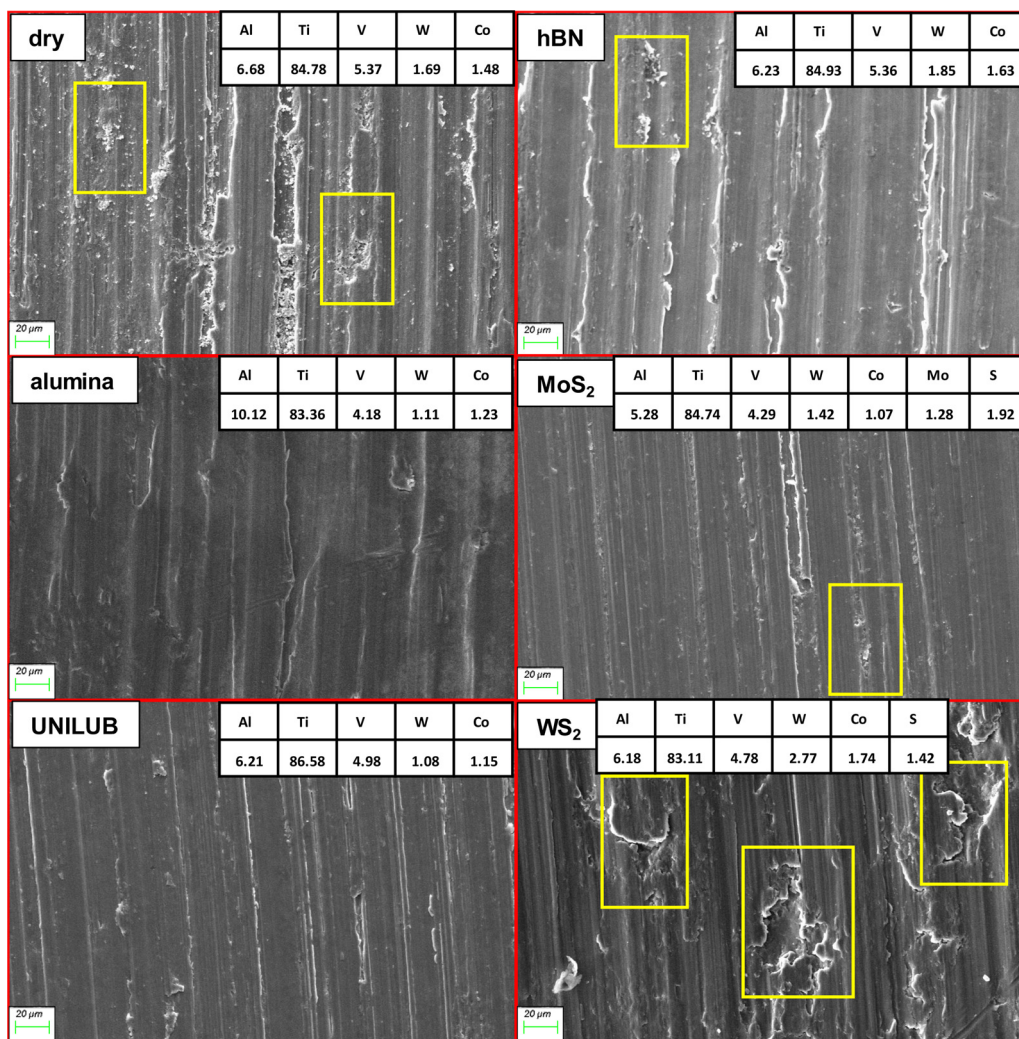


Fig. 10. SEM images of the wear tracks under different lubricating conditions at 100 ml/hr flow rate. Elemental composition (in %) on the surfaces is given in the inset tables.

variations in the coefficient of friction observed in Fig. 8. Lower wear depth and specific wear indicate better anti-wear properties. At 100 ml/hr, the reduction in specific wear for alumina nanofluid and the commercial lubricant are 37.03 % and 40.16 % respectively as compared to dry friction, and the reduction in wear track depth for alumina nanofluid and the commercial lubricant are 23.4 % and 28.37 % respectively as compared to dry friction. It can be inferred from Fig. 9 that the commercial lubricant has the best anti-wear properties, closely followed by alumina nanofluids. Alumina nanofluids, even though are effective in reducing the coefficient of friction, are not as effective as the commercial lubricant in controlling wear. This can be attributed to abrasion between the nanoparticles and the sliding surface [38]. hBN, MoS₂, and WS₂ nanofluids performed worse than alumina nanofluids, with wear at 6 ml/hr similar to that of dry sliding.

Fig. 10 shows the SEM images of the wear tracks under dry friction and different fluids at 100 ml/hr flow rate. Surface damage is shown in the boxes inset in Fig. 10. Dry sliding has caused the highest surface damage due to lack of lubrication and the direct contact between sliding surfaces leading to increased wear. The anti-friction and anti-wear properties of alumina nanofluids can be confirmed by the minimal presence of surface damage like scratches and plastic deformation on the surface. This can be attributed to the polishing effect of the spherical alumina nanoparticles which reduces surface damage [39]. The commercial lubricant has also shown good anti-friction and anti-wear properties as can be seen on the worn surface with a small amount of surface damage. The presence of alumina in the asperities of the surface as explained earlier can be confirmed by the elemental composition of the surface by EDS as shown in the inset table in Fig. 10. hBN, MoS₂, and WS₂ nanofluids have failed to significantly decrease friction and wear of the surface. The structure of these materials is lamellar in which the layers are held together by weak Van der Waals force. The lubricating mechanism is by the sliding of the layers [40] which has provided some amount of lubrication in the present study, but not as adequately as alumina nanofluids. The findings are in agreement with the measured coefficient of friction, wear depth and specific wear as shown in Fig. 8 and Fig. 9.

Micromilling experiments

Micromilling experiments were conducted on Ti-6Al-4V to evaluate the machining performance of the prepared nanofluids in minimum quantity lubrication (MQL) mode at different flow rates. The schematic of the micromilling operation showing the direction of forces is shown in Fig. 11a. Fig. 11b is a plot showing the typical nature of cutting forces. Feed force (F_x) is the force along the feed direction of the cutting tool, transverse force (F_y) is the force perpendicular to the direction of feed i.e. the force acting on the side walls of the micro-channels, and thrust force (F_z) is the vertical force acting along the axis of the cutting tool.

The variations in all the three cutting forces under different lubricating conditions are shown in Fig. 12. RMS values of the measured cutting forces were used for plotting and the error bars represent the standard deviation in the forces. All the cutting forces show a trend similar to that of the coefficient of friction shown in Fig. 8. Cutting forces for dry milling are the highest, and for the commercial lubricant, cutting forces are the least at all the flow rates. Cutting forces for alumina nanofluids are close to those for the commercial lubricant with feed force (F_x) being up to 8% higher, transverse force (F_y) being up to 12.8 % higher, and thrust force (F_z) being up to 9.5 % higher than the commercial lubricants at a cutting velocity of 60 m/min. hBN, MoS₂, and WS₂ nanofluids were not as effective as alumina nanofluid in reducing the cutting forces. This significant reduction in cutting forces using alumina nanofluids can be attributed to both the nano ball-bearing effect of the spherical alumina nanoparticles and the entrapment of the nanoparticles in the asperities of the workpiece, thereby reducing friction [19–22,24]. Further, the reduction in the forces was

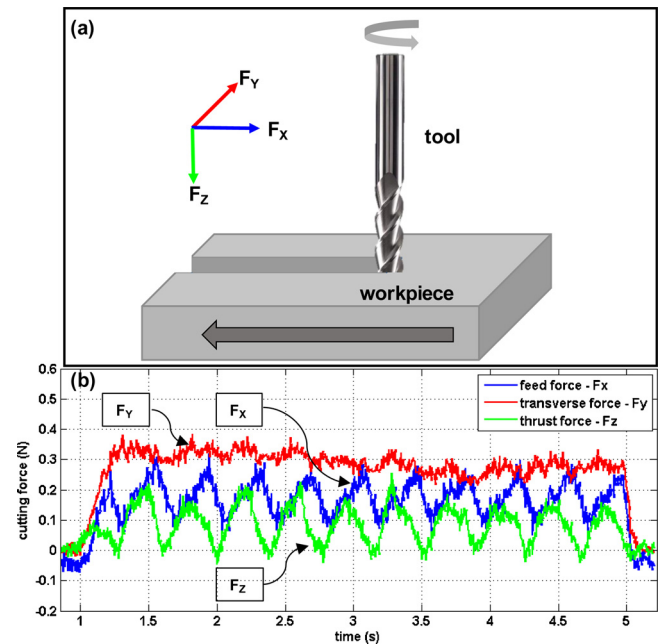


Fig. 11. Typical cutting forces in micromilling (a) measured in three directions and (b) force data as processed in MATLAB.

observed to be higher when the flow rate was increased from 50 to 100 ml/hr than when the flow rate was increased from 6 to 50 ml/hr for all the lubricants used. This can be attributed to the increase in tribofilm stability and the higher availability of nanoparticles at 100 ml/hr as explained from the tribology experiments. Further, the cutting forces are observed to increase with an increase in the cutting velocity from 10 m/min to 60 m/min. This can be attributed to the strain hardening effect at higher cutting velocities. Johnson-Cook material model states the flow stress for a material as a function of strain, strain rate, and temperature as given in Eq. (1).

$$\sigma = \left(A + B\varepsilon^n \right) \left(1 + C \ln \left(\frac{\dot{\varepsilon}}{\dot{\varepsilon}_o} \right) \right) \left(1 + \left(\frac{T - T_o}{T_m - T_o} \right)^m \right) \quad (1)$$

where A is the material yield stress constant, B is the hardening module of the material, C is the strain rate susceptibility, n is the hardening coefficient, and m is the thermal softening coefficient of the material. Other parameters are: ε is the plastic strain, $\dot{\varepsilon}$ is the strain rate (s^{-1}), $\dot{\varepsilon}_o$ is the reference strain rate (s^{-1}), T is the workpiece temperature, T_o is the room temperature, and T_m is the workpiece melting temperature. J-C constants for Ti-6Al-4V are given in Table 5 [41–43], and material properties are given in Table 6 [44].

Strain rate is a function of cutting velocity as shown in Eq. (2).

$$\dot{\varepsilon} = \frac{v_c \cos(\gamma_o)}{\cos(\beta - \gamma_o) \Delta y} \quad (2)$$

where v_c is the cutting velocity, γ_o is the orthogonal rake angle of the tool (5°), β is the shear plane angle, and Δy is the adiabatic shear band thickness. It can be seen that the strain rate increases by 6 fold as the cutting velocity increases from 10 m/min to 60 m/min. The temperature rise is not high enough in micro-scale machining to cause significant strain-softening effects as compared to meso-scale machining for the above range of cutting velocities [45], and hence, the temperature softening effects can be safely neglected. From Eq. (1), an increase in strain rate can contribute to the rise in flow stress, thereby increasing the cutting forces at 60 m/min cutting velocity.

Fig. 13 shows a typical micromilled channel. The upmilling and downmilling sides and the measurement strategy for the top burr are shown. Top burr width was measured at multiple locations in both

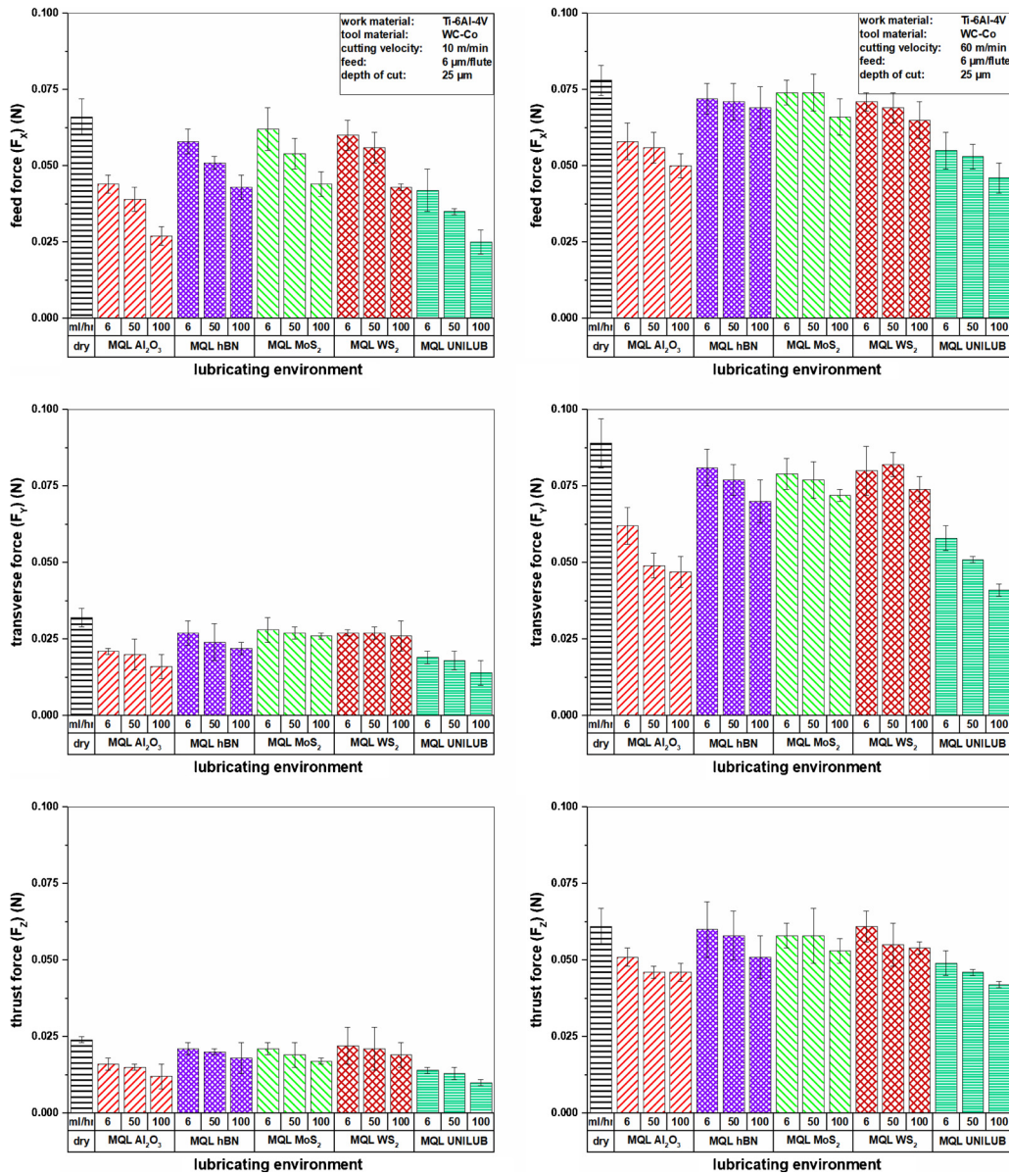


Table 5
Johnson-Cook constants for Ti-6Al-4 V [41–43].

A	B	C	m	n
1098	1092	0.014	1.1	0.93

Table 6
Physical properties of Ti-6Al-4 V [44].

Property	Value
Density (g/cm ³)	4.43
Young's modulus (GPa)	113.8
Poisson's ratio	0.342
Yield strength (MPa)	1098
Shear strength (MPa)	550
Melting temperature (°C)	1600

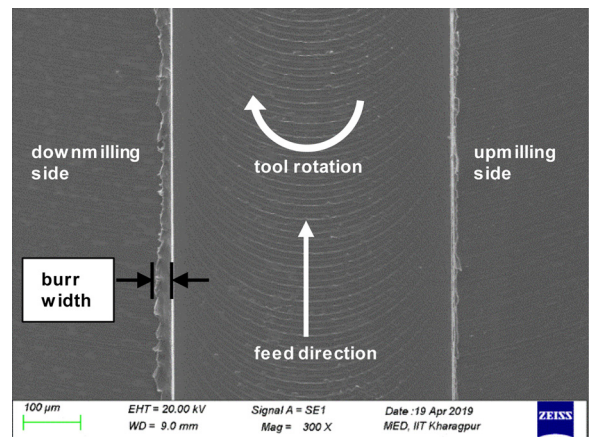


Fig. 13. Typical micro-channel showing the workpiece feed direction, down-milling and upmilling sides, and burr width measurement.

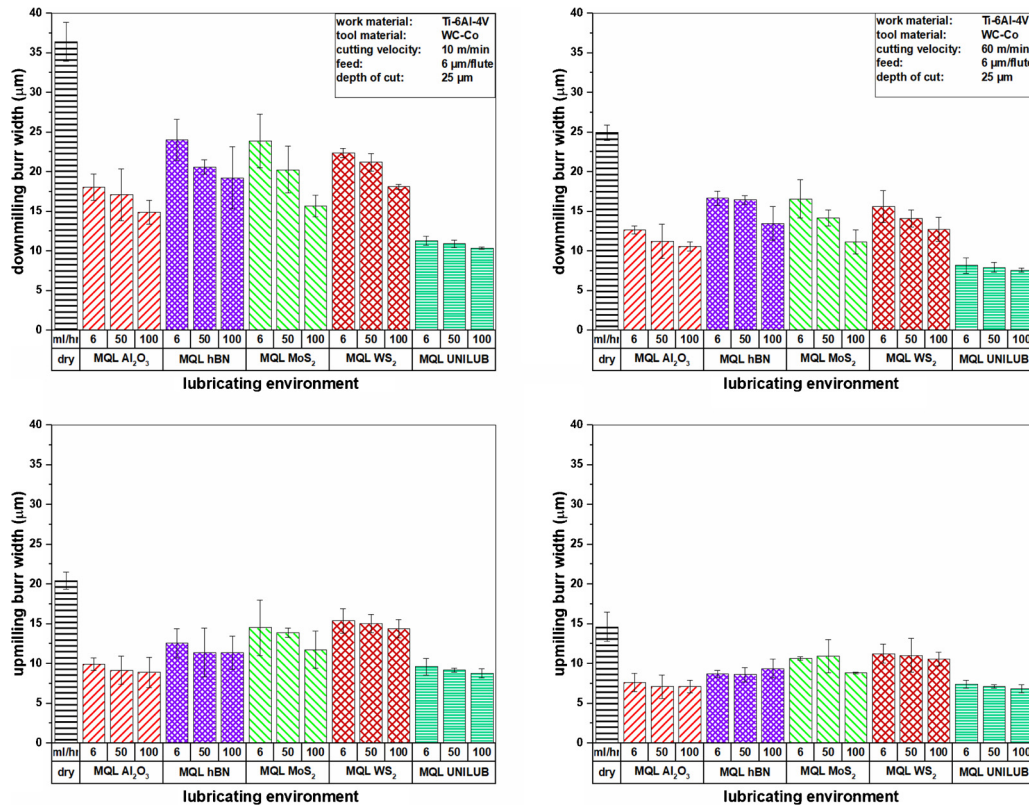


Fig. 14. Variations in downmilling and upmilling burr width under different lubricating conditions.

downmilling and upmilling sides and averaged. The variations in burr width under different lubricating conditions are shown in Fig. 14. Burr width was measured at six different locations each in both downmilling and upmilling directions and averaged. Error bars represent the standard deviation in the burr width. It is well known that in micromilling, ploughing and rubbing of the tool edge against the workpiece surface have a higher contribution than that in meso-scale machining. This phenomenon, known as size effect, has been studied extensively [7,46–50]. More ploughing and rubbing are known to cause higher burr formation [50]. The large top burrs in micromilling due to size effect has been explained by Bissacco et.al [4]. Very high biaxial compressive stress pushes material toward the free surface and generates large top burrs. It can be seen that the commercial lubricant has resulted in the smallest burrs in both downmilling and upmilling directions. This can be attributed to the better anti-friction and anti-wear properties of the commercial lubricant. Similarly, alumina has better anti-friction and anti-wear characteristics as compared to the other nanofluids, which has resulted in smaller burrs. Thus, a relation can be established between friction and burr formation in micromilling based on the above results. hBN, MoS₂, and WS₂ were not as effective as alumina nanofluids or the commercial lubricant owing to their less effectiveness in reducing friction. It is observed that the downmilling burrs are larger than upmilling burrs in all the cases. This is consistent with similar reports from literature [7,51–53]. Ravi et.al have explained this trend in micromilling [51]. They have observed that in the downmilling side, burrs are broken at a distance away from the root of the burr, while in the upmilling side, burrs are broken at the root of the burr. This results in larger burrs on the downmilling side than on the upmilling side. Further, both downmilling and upmilling burrs tend to be smaller at higher cutting velocity. In micromilling, where feed per tooth is comparable to the tool edge radius, ploughing and rubbing dominate the machining mechanism. In such cases, the tool wear decreases at higher cutting velocities as explained by Lee and Dornfeld [3]. They have observed that in micromilling, built-up edge tends to remain on the tool for

longer and the rate of wear decreases as the cutting velocity increases. This can explain the decrease in burr size at higher cutting velocities.

Conclusions

The lubrication ability of different water-based nanofluids in minimum quantity lubrication (MQL) mode has been studied. Water-based alumina, hBN, MoS₂, and WS₂ nanofluids have been prepared and their anti-friction and anti-wear properties have been studied using ball-on-disk tribometry at different flow rates in MQL mode. The results are compared with a commercial lubricant (UNILUB 2032). Micromilling experiments were performed on Ti-6Al-4V using the prepared nanofluids in MQL mode. The following conclusions can be drawn based on the experimental results.

- Alumina nanofluids have shown the best anti-friction and anti-wear properties among all the nanofluids tested due to their spherical shape, which causes a ball bearing effect and reduces friction.
- Alumina nanoparticles also fill in the asperities in the workpiece surface due to their spherical shape, further reducing the contact between the sliding surfaces, thereby reducing friction and wear. This can be confirmed from the EDS of the wear tracks.
- The commercial lubricant has shown the best anti-friction and anti-wear performance due to the formation of a stable tribofilm by the commercial lubricant as compared to the nanofluids.
- An increase in flow rate further reduced friction and wear. This is due to the increase in the tribofilm stability and the increased availability of the nanoparticles, both of which tend to reduce friction and wear.
- Solid lubricant based nanofluids like hBN, MoS₂, and WS₂ have shown slight improvement in anti-friction and anti-wear properties, but could not perform as better as the spherical alumina nanoparticles.
- The variations in all the three cutting forces have shown a similar

trend as that of the coefficient of friction under different lubricating conditions. Commercial lubricant performed the best, closely followed by alumina nanofluids.

- Downmilling and upmilling burr width were measured in all the cases and it is found that the commercial lubricant and alumina nanofluids have shown superior performance in reducing the burr width. This can be attributed to the better anti-friction properties of these fluids, which can reduce friction, thereby reducing the ploughing and rubbing between the tool and the workpiece resulting in a reduction in the burr width.
- Alumina nanofluids and the commercial lubricant have shown significant reduction in machining forces and burr formation as compared to the other nanofluids. This is in correlation to the tribological performance of these cutting fluids.
- From the experimental results, it can be concluded that water-based alumina nanofluids can be a viable alternative for conventional cutting fluids in micro-machining of Ti-6Al-4 V.

Funding

The authors received no financial support for the research, authorship, and/or publication of this article.

Declaration of Competing Interest

The authors declare that they have no known competing financial interests or personal relationships that could have appeared to influence the work reported in this paper.

References

- [1] Llanos I, Agirre A, Urreta H, Thepsonthi T, Ozel T. Micromilling high aspect ratio features using tungsten carbide tools. *Proc Inst Mech Eng Part B J Eng Manuf* 2014;228:1350–8. <https://doi.org/10.1177/0954405414522214>.
- [2] Agirre A, Thepsonthi T, Özel T. Micro-milling of metallic thin-wall features with applications in micro-heat sinks. *Ninth International Conference on HIGH SPEED MACHINING* 2012.
- [3] Lee K, Dornfeld DA. Micro-burr formation and minimization through process control. *Precis Eng* 2005;29:246–52. <https://doi.org/10.1016/j.precisioneng.2004.09.002>.
- [4] Bissacco G, Hansen HN, De Chiffre L. Micromilling of hardened tool steel for mould making applications. *J Mater Process Technol* 2005;167:201–7. <https://doi.org/10.1016/j.jmatprotec.2005.05.029>.
- [5] DeVor R, Ehmman K, Kapoor S. *Technology assessment on current advanced research in micro-machining and related areas*. McLean, VA, USA: The Association For Manufacturing Technology; 2004. p. 239.
- [6] Koç M, Özel T. *Micro-manufacturing: design and manufacturing of micro-products*. John Wiley & Sons; 2011.
- [7] Lee K, Dornfeld DA. An experimental study on burr formation in micro-milling aluminium and copper. *Transactions of NAMRI/SME*; 2002. p. 1–8.
- [8] Cheng J, Jin Y, Wu J, Wen X, Gong Y, Shi J, et al. Experimental study on a novel minimization method of top burr formation in micro-end milling of Ti-6Al-4V. *Int J Adv Manuf Technol* 2016. <https://doi.org/10.1007/s00170-015-8312-7>.
- [9] Criteria for a recommended standard: occupational exposure to metalworking fluids. 2018. <https://doi.org/10.26616/NIOSH/PUB98102>.
- [10] Adler DP, Hii WW-S, Michalek DJ, Sutherland JW. Examining the role of cutting fluids in machining and efforts to address associated Environmental/Health concerns. *Mach Sci Technol* 2006;10:23–58. <https://doi.org/10.1080/10910340500534282>.
- [11] Çakır A, Yağmur S, Kavak N, Küçükçürük G, Şeker U. The effect of minimum quantity lubrication under different parameters in the turning of AA7075 and AA2024 aluminium alloys. *Int J Adv Manuf Technol* 2015. <https://doi.org/10.1007/s00170-015-7878-4>.
- [12] Sun J, Wong YS, Rahman M, Wang ZG, Neo KS, Tan CH, et al. Effects of coolant supply methods and cutting conditions on tool life in end milling Titanium Alloy. *Mach Sci Technol* 2006;10:355–70. <https://doi.org/10.1080/10910340600902181>.
- [13] Anand N, Kumar AS, Paul S. Effect of cutting fluids applied in MQCL mode on machinability of Ti-6Al-4V. *J Manuf Process* 2019;43:154–63. <https://doi.org/10.1016/j.jmapro.2019.05.029>.
- [14] Narutaki N, Murakoshi A, Motonishi S, Takeyama H. Study on machining of titanium alloys. *CIRP Annals* 1983;32:65–9. [https://doi.org/10.1016/S0007-8506\(07\)63362-9](https://doi.org/10.1016/S0007-8506(07)63362-9).
- [15] Vazquez E, Kemmoku DT, Noritomi PY, da Silva JVL, Ciurana J. Computer Fluid Dynamics Analysis for Efficient Cooling and Lubrication Conditions in Micromilling of Ti6Al4V Alloy. *Mater Manuf Process* 2014;29:1494–501. <https://doi.org/10.1080/10426914.2014.941864>.
- [16] Ziberov M, da Silva MB, Jackson M, Hung WNP. Effect of cutting fluid on micro-milling of Ti-6Al-4V titanium alloy. *Procedia Manuf* 2016;5:332–47. <https://doi.org/10.1016/j.promfg.2016.08.029>.
- [17] Choi SUS, Eastman JA. *Enhancing thermal conductivity of fluids with nanoparticles*. ASME-Publications-Fed 1995;231:99–106.
- [18] Xie H, Wang J, Xi T, Liu Y, Ai F, Wu Q. Thermal conductivity enhancement of suspensions containing nanosized alumina particles. *J Appl Phys* 2002;91:4568. <https://doi.org/10.1063/1.1454184>.
- [19] Jiao D, Zheng S, Wang Y, Guan R, Cao B. The tribology properties of alumina/silica composite nanoparticles as lubricant additives. *Appl Surf Sci* 2011;257:5720–5. <https://doi.org/10.1016/j.apsusc.2011.01.084>.
- [20] Mao C, Huang Y, Zhou X, Gan H, Zhang J, Zhou Z. The tribological properties of nanofluid used in minimum quantity lubrication grinding. *Int J Adv Manuf Technol* 2014;71:1221–8. <https://doi.org/10.1007/s00170-013-5576-7>.
- [21] Tao X, Jiazhang Z, Kang X. The ball-bearing effect of diamond nanoparticles as an oil additive. *J Phys D Appl Phys* 1996;29:2932–7. <https://doi.org/10.1088/0022-3727/29/11/029>.
- [22] Kong L, Sun J, Bao Y. Preparation, characterization and tribological mechanism of nanofluids. *RSC Adv* 2017;7:12599–609. <https://doi.org/10.1039/C6RA28243A>.
- [23] Teng T-P, Hung Y-H. Estimation and experimental study of the density and specific heat for alumina nanofluid. *J Exp Nanosci* 2014;9:707–18. <https://doi.org/10.1080/17458080.2012.696219>.
- [24] Zhao C, Chen YK, Ren G. A study of tribological properties of water-based Ceria nanofluids. *Tribol Trans* 2013;56:275–83. <https://doi.org/10.1080/10402004.2012.748948>.
- [25] Zhao J, He Y, Wang Y, Wang W, Yan L, Luo J. An investigation on the tribological properties of multilayer graphene and MoS₂ nanosheets as additives used in hydraulic applications. *Tribol Int* 2016;97:14–20. <https://doi.org/10.1016/j.triboint.2015.12.006>.
- [26] Sahoo RR, Biswas SK. Deformation and friction of MoS₂ particles in liquid suspensions used to lubricate sliding contact. *Thin Solid Films* 2010;518:5995–6005. <https://doi.org/10.1016/j.tsf.2010.05.127>.
- [27] Liao YS, Yu YP, Chang CH. Effects of cutting fluid with nano particles on the grinding of titanium alloys. *Adv Mat Res* 2010;126–128:353–8. <https://doi.org/10.4028/www.scientific.net/AMR.126-128.353>.
- [28] Setti D, Sinha MK, Ghosh S, Venkateswara Rao P. Performance evaluation of Ti-6Al-4V grinding using chip formation and coefficient of friction under the influence of nanofluids. *Int J Mach Tools Manuf* 2015;88:237–48. <https://doi.org/10.1016/j.ijmactools.2014.10.005>.
- [29] Kim DH, Lee P-H, Kim JS, Moon H, Lee SW. Experimental Study on Micro End-Milling Process of Ti-6Al-4V Using Nanofluid Minimum Quantity Lubrication (MQL). Volume 1: Materials; Micro and Nano Technologies; Properties, Applications and Systems; Sustainable Manufacturing, ASME, 2014; p. V001T03A015. <https://doi.org/10.1115/MSEC2014-4124>.
- [30] Aluminum Oxide Nanopowder; MSDS no NS6130-03-300. Nanoshel LLC; 2020. n.d. <https://www.nanoshel.com/admin/DownloadPDF/download/206/MSDS>.
- [31] Boron Nitride Nanopowder; MSDS no NS6130-02-260. Nanoshel LLC; 2020. n.d. <https://www.nanoshel.com/admin/DownloadPDF/download/312/MSDS>.
- [32] Molybdenum Disulphide Nanopowder; MSDS no NS6130-02-242. Nanoshel LLC; 2020. n.d.
- [33] Tungsten Disulphide Nanopowder; MSDS no NS6130-02-243. Nanoshel LLC; 2020. n.d. <https://www.nanoshel.com/admin/DownloadPDF/download/270/MSDS>.
- [34] Hertz H. Über die berührung fester elastische Körper und über die Harte. *Verhandlungen Des Vereins Zur Beförderung Des Gewerbefleisses*; 1982. n.d.
- [35] Boyde S. Hydrolytic stability of synthetic ester lubricants. *J Synth Lubr* 2000;16:297–312. <https://doi.org/10.1002/jsl.3000160403>.
- [36] Suda S, Yokota H, Inasaki I, Wakabayashi T. A synthetic ester as an optimal cutting fluid for minimal quantity lubrication machining. *CIRP Annals* 2002;51:95–8. [https://doi.org/10.1016/S0007-8506\(07\)61474-7](https://doi.org/10.1016/S0007-8506(07)61474-7).
- [37] Wakabayashi T, Inasaki I, Suda S, Yokota H. Tribological characteristics and cutting performance of lubricant esters for semi-dry machining. *CIRP Annals* 2003;52:61–4. [https://doi.org/10.1016/S0007-8506\(07\)60531-9](https://doi.org/10.1016/S0007-8506(07)60531-9).
- [38] Gara L, Zou Q. Friction and wear characteristics of water-based ZnO and Al₂O₃ nanofluids. *Tribol Trans* 2012;55:345–50. <https://doi.org/10.1080/10402004.2012.656879>.
- [39] Wang Y, Li C, Zhang Y, Li B, Yang M, Zhang X, et al. Experimental evaluation of the lubrication properties of the wheel/workpiece interface in MQL grinding with different nanofluids. *Tribol Int* 2016;99:198–210. <https://doi.org/10.1016/j.triboint.2016.03.023>.
- [40] Rahmati B, Sarhan AAD, Sayuti M. Morphology of surface generated by end milling Al6061-T6 using molybdenum disulfide (MoS₂) nanolubrication in end milling machining. *J Clean Prod* 2014;66:685–91. <https://doi.org/10.1016/j.jclepro.2013.10.048>.
- [41] Lesuer DR. *Experimental investigations of material models for Ti-6Al-4V titanium and 2024-T3 aluminum*. 2000.
- [42] Özel T, Zeren E. Determination of work material flow stress and friction for FEA of machining using orthogonal cutting tests. *J Mater Process Technol* 2004;153–154:1019–25. <https://doi.org/10.1016/j.jmatprotec.2004.04.162>.
- [43] Yadav AK, Kumar M, Bajpai V, Singh NK, Singh RK. FE modeling of burr size in high-speed micro-milling of Ti6Al4V. *Precis Eng* 2017. <https://doi.org/10.1016/j.precisioneng.2017.02.017>.
- [44] Zhang WJ, Reddy BV, Deevi SC. Physical properties of TiAl-base alloys. *Scr Mater* 2001;45:645–51. [https://doi.org/10.1016/S1359-6462\(01\)01075-2](https://doi.org/10.1016/S1359-6462(01)01075-2).
- [45] Dhanorkar A, Ozel T. Meso/micro scale milling for micro-manufacturing. *Int J Mechatron Manuf Syst* 2008.

- [46] de Oliveira FB, Rodrigues AR, Coelho RT, de Souza AF. Size effect and minimum chip thickness in micromilling. *Int J Mach Tools Manuf* 2015;89:39–54. <https://doi.org/10.1016/j.ijmachtools.2014.11.001>.
- [47] Bissacco G, Hansen HN, Slunsky J. Modelling the cutting edge radius size effect for force prediction in micro milling. *CIRP Annals* 2008;57:113–6. <https://doi.org/10.1016/j.cirp.2008.03.085>.
- [48] Kim C-J, Bono M, Ni J. Experimental analysis of chip formation in micro-milling. *Technical papers-society of manufacturing engineers-all series*. 2002.
- [49] Biermann D, Kahnis P. Analysis and simulation of size effects in micromilling. *Prod Eng* 2010;4:25–34. <https://doi.org/10.1007/s11740-009-0201-1>.
- [50] Dix M. Modelling, simulations and experimental verification of size effects in burr formation. *Proc. 2nd ICNFT, 2007* 2007.
- [51] Lekkala R, Bajpai V, Singh RK, Joshi SS. Characterization and modeling of burr formation in micro-end milling. *Precis Eng* 2011;35:625–37. <https://doi.org/10.1016/j.precisioneng.2011.04.007>.
- [52] Kiswanto G, Zariatn DLL, Ko TJJ. The effect of spindle speed, feed-rate and machining time to the surface roughness and burr formation of Aluminum Alloy 1100 in micro-milling operation. *J Manuf Process* 2014;16:435–50. <https://doi.org/10.1016/j.jmapro.2014.05.003>.
- [53] Li K-M, Chou S-Y. Experimental evaluation of minimum quantity lubrication in near micro-milling. *J Mater Process Technol* 2010;210:2163–70. <https://doi.org/10.1016/j.jmatprotec.2010.07.031>.